Usage guidelines

Delay Compensated State Estimation for Telepresence Robot Navigation

Barnali Das*, Gordon Dobie

Department of Electronic and Electrical Engineering,
University of Strathclyde, Glasgow, Scotland, United Kingdom

Abstract

Telepresence robots empower human operators to navigate remote environments. However, operating and navigating the robot in an unknown environment is challenging due to delay in the communication network (*e.g.,* distance, bandwidth, communication drop-outs etc.), processing delays and slow dynamics of the mobile robots resulting in time-lagged in the system. Also, erroneous sensor data measurement which is important to estimate the robot's true state (positional information) in the remote environment, often create complications and make it harder for the system to control the robot. In this paper, we propose a new approach for state estimation assuming uncertain delayed sensor measurements of a Telepresence robot during navigation. A new real world experimental model, based on Augmented State Extended Kalman Filter (AS-EKF), is proposed to estimate the true position of the Telepresence robot. The uncertainty of the delayed sensor measurements have been modelled using probabilistic density functions (PDF). The proposed model was successfully verified in our proposed experimental framework which consists of a state-of-the-art differential-drive Telepresence robot and a motion tracking multi-camera system. The results show significant improvements compared to the traditional EKF that does not consider uncertain delays in sensor measurements. The proposed model will be beneficial to build a real time predictive display by reducing the effect of visual delay to navigate the robot under the operator's control command, without waiting for delayed sensor measurements.

Keywords: State estimation, delay compensation, telepresence, robot navigation, AS-EKF.

1. Introduction

A Telepresence system is a set of technology which gives the appearance of being present, at a place other than their true location. Telepresence allows a human operator to control and navigate a mobile robot around the remote environment and in many cases interact

---

with their audiences through video conferencing [1]. In general, a Telepresence system is composed of a local site (where a human operator drives a hand-controller device); a remote site (where a mobile robot interacts with the physical world); and a communication channel that links both sites. A Telepresence robot provides interactive two-way audio and video communication with a remote sender and a receiver for building a communication system between the two people in different places. These systems, which are primarily used in the context of promoting social interaction between people, became popular in many emerging applications including hospitals and healthcare consultations, remote co-working in office spaces, tour guidance, security and surveillance (*e.g.,* remote night watch person[1]), factory inspection, instructor led educations and many more.

Telepresence robots suffer significant challenges during navigation in the remote site due to varying communication time delays [2] frequently caused by the present state of the network as depicted in Figure 1. Moreover, the distance between the human operator and remote sites of a Telepresence system introduces time varying delays adding distortion in the reference commands and feedback signals resulting in instability or poor performance of the system. The time elapsed between making an action decision and perceiving the consequences of that action in the environment introduces control delay. Therefore, it is advantageous to compensate such delays for robust navigation of a Telepresence robot. A predictive display is also be helpful to address the challenges of visual mismatch between the predicted state and actual navigation state of the robot.
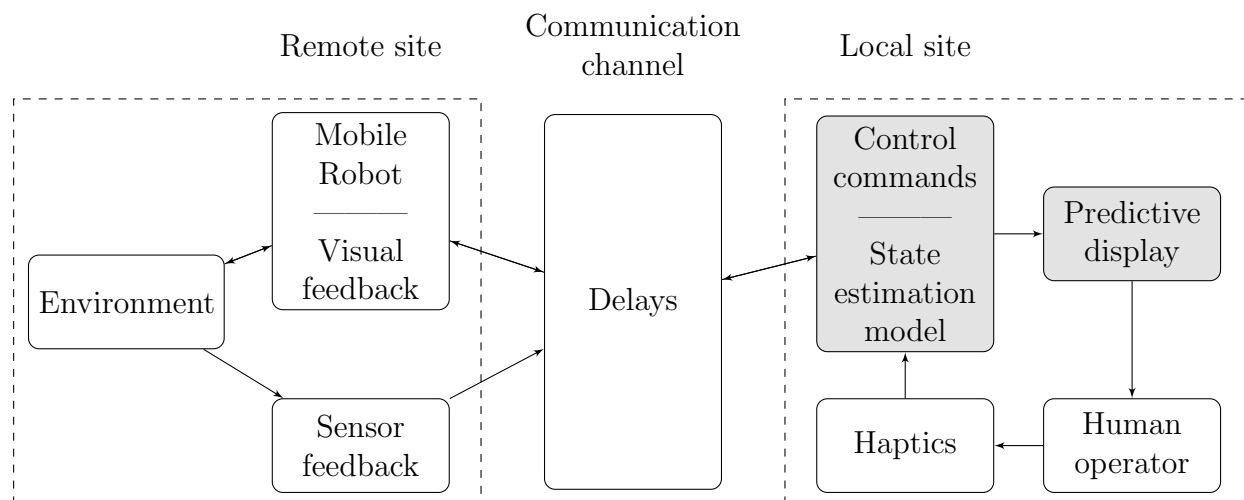

Figure 1: A brief architecture of the Telepresence system with introducing uncertain time varying communication delay.

This paper proposes a new approach for state estimation that can model and compensate such delays using uncertain delayed sensor measurements in Telepresence robot navigations. We hypothesized multiple augmented states in the proposed approach to estimate the true

---

[1]https://www.knightscope.com//

position of a commercially available differential drive Telepresence robot. The uncertainty of the delayed sensor measurement was modelled using a probabilistic density functions (PDF). This is particularly challenging specially for a differential drive robot where additional system errors occur due the kinematics of individual wheels. While there have been several attempts to address the delay problem in mobile robots and tele operated systems, to the best knowledge of the authors this is the first time such a hypothesis is applied on a commercially available differential drive Telepresence robot in a real environment experimental framework.

2. Background and contributions

2.1. Delay modelling in Telepresence systems

Although several methods and algorithms were proposed to address such time delay problem in the Telepresence (also known as *Tele-operated*) systems it is still an open issue that needs to be addressed. The presence of time delay causes instability in the system and poor performance of the robot navigation. In this subsection we described few efforts of the time delay compensation methods in the Telepresence systems.

Kawabata *et al.* [3] have proposed a framework of human interface systems for tele-operation to achieve smooth operation of a mobile robot through a communication link, considering time delays in data transfer. The prototype of the teleoperation system was constructed utilizing the virtual world as an operation interface. Colledanchise *et al.* [4] have also showed how to use event based sampling to reduce the number of measurements done, thereby saving time, computational resources and power, without jeopardizing critical system properties such as safety and goal convergence.

Anderson and Vittorias *et al.* [5, 6] have introduced a new control law for controlling a teleoperator with time delay, which achieved stability for the teleoperator independent of time delay in the system. The model based on the scattering theory, which allows the transmission and encoding of haptic data in time delayed teleoperation systems. Funda *et al.* [7, 8] in his research proposed a new control methodology, called teleprogramming, which allows for efficient control of a robotic system in the presence of significant feedback delays without substantial degradation in the overall system performance. A teleprogramming system allows the operator to kinesthetically as well as visually interact with a graphical simulation of the remote environment and to interactively, on-line teleprogram the remote manipulator through a sequence of elementary symbolic instructions.

An important feature Telepresence system is a possibility transmission delay and data packet drop-outs over the Internet. If a significant amount of time elapsed or data is dropped due to network congestion, it may result in discontinuity of the reference trajectories and the forces transmitted between the master and the slave. Brady *et al.* [9] developed a new robot controlling model where communication propagation delays exist over the internet. This model is flexible enough to embrace the wide variety of possible communication mediums for remote teleoperation. Mora *et al.* [10] presented a novel method combining the visualization of two models of the mobile robot inside a 3D virtual environment. One model represents the position and orientation provided by real time GPS located on the robot and another model

is based on inputs given by human operator through the information gathered by the laser range finder sensor to deal with the time delay and narrow bandwidth limitations. While, Hu *et al.* [11] introduced a 3D model based predictive display system where the operator sees the predicted image instead of delayed video to control a robot remotely. Natori *et al.* [12] have presented a effective time delay compensation method based on the concept of network disturbance and communication disturbance observer for bilateral teleoperation systems under time varying delay. They validated the time delay compensation method for both the cases of constant delay and time varying delay with Smith predictor.

Bejczy *et al.* [13, 14] have developed a predictive display system based on high-fidelity real-time graphics overlay for use in time-delayed telemanipulation. Human-assisted camera calibration techniques were also developed for an exact alignment of the graphics image with the actual camera view. Slawinski *et al.* [15] have proposed a predicted control scheme applied to teleoperation of a mobile robot with force feedback and time-varying delay. While the user receives delayed force and generates delayed commands permanently, the scheme predicts the users intention and fuses such commands with a stable controller in order to achieve a collision-free trajectory of the mobile robot.

In this paper, we aim to address issues related to time delay effecting robot state estimation in the remote site from the local site. At this juncture, it is worth noting that we envisage to build a predictive display system at the local site to help the human operator to navigate the mobile robot with time-varying delayed measurement and the proposed system aimed to support real-time robot position tracking and immediate control at the human operator site. As the mobile robot is controlled by a human operator through a communication network in a remote site, the human operator should know the robot's pose to control the robot smoothly. If the time delays are not compensated to estimate the robot pose correctly in the remote site, the human operator may cause an accident crashing obstacles because of the robot pose which the operator inaccurately recognised. Therefore, we designed a non-linear state estimation computational model to estimate the robot's true state by incorporating a new approach for delay compensation.

2.2. State estimation to compensate time delay in the navigation

The state of a robot is a set of position, orientation and velocity, which is the robots motion over time. This includes estimation of the state of the robot's kinematic system by combining knowledge from a priori information and sensor measurements. State estimation in dynamical systems is crucial in real-world applications as the true state is unknown and sensors have a limited precision, therefore, provide only a sequence of uncertain noisy measurements. Commonly used state estimation methods to stabilize non-linear delayed system include filtering methods [16, 17] or predictor feedback control theory [18, 19]. Among them filtering methods such as the Extended Kalman Filter (EKF) are commonly used in robot navigation to acquire an estimate of the true state from noisy measurements. However, when a filtering processor is connected to a sensor through a network, there is a fundamental communication time. Moreover, if raw sensor data require post-processing, in order to update the state of the dynamical system, additional post-processing time is needed, resulting in a delay between the acquisition of a measurement and its availability to the filter.

4

If the time delay is known, the past state can be predicted applying backward prediction of the current state. Bar-Shalom [20] proposed an optimal and suboptimal algorithm for one step delayed measurement. The extended version for multi-step delayed measurements also proposed in [21]. In case of a non-linear system, it needs modifications for state estimation. Larsen *et al.* [22] introduced a method based on extrapolation of a delayed measurement to the present time using past and present estimates of the Kalman Filter. An extension algorithm of [22] is proposed in [23] that interpolating a delayed measurement minimizes the computational time even for significant time delays.

State augmentation has also been used in time delayed measurement. Delayed measurement directly corrects the past state and a new prediction of the current state is then obtained from the corrected past state. Challa *et al.* [24] presented a Bayesian solution to the out of sequence measurement (OOSM) problem and provided approximate, implementable algorithms for both cluttered and non-cluttered scenarios involving single and multiple time-delayed measurement. Van Der Merwe *et al.* [25] applied the sigma point Kalman Filter instead of EKF to the augmented technique to fuse latency lagged observations for non-linear estimation and multiple sensors fusion.

If there is uncertainty in measurement delay, it is hard to predict because the measured time delay may have noise. Julier and Uhlmann [26] suggested a covariance union algorithm for accommodating time step uncertainty directly into the observation covariance so that filter consistency is always maintained. Jun *et al.* [27] proposed event based filtering for time-varying non-linear systems that uses probabilities to address uncertain missing measurements. A recursive filtering algorithm is proposed by Zou *et al.* [28] targetting a class of linear time-varying systems of networked sensors for robust signal transmission. Within the scope, this paper only focuses on estimating uncertain time delays for robot navigation. The underlying assumption in such cases is that if the time delay is able to be modelled as a form of a distribution, the uncertainty of delay can be modelled. Challa *et al.* [24] proposed a probabilistic data association filter to deal with data association issues arising from the presence of clutter in the OOSM problem. Choi *et al.* [29] proposed a state estimation algorithm incorporating uncertainty of measurement delay. By modelling uncertain delay as a probabilistic density function is accounted for by the proposed estimator, combined with the augmented state Kalman Filter. However, the majority of these algorithms reported simulation only results that neither considered a real environment nor the techniques were applied on a real robot.

2.3. Our contributions

While state estimation with augmentation methods have been proposed in the literature, they were not applied in Telepresence navigation. Only exception is Choi *et al.* [29] where the authors simulated their algorithms with an intention to apply on Telepresence robot navigation. However, a real life scenario poses many other additional challenges including system errors, mechanical errors relating to robot kinematics. In addition to this, a differential drive robot (our chosen state-of-the-art industrial Telepresence robot) imposes additional complexities mainly due to individual wheels controls impacting the robot kinematics.

To address this we propose an experimental model for state estimation for navigation of Telepresence robots with uncertain and delayed sensor measurements in a non-linear system. We hypothesised and developed the approach by introducing augmented states into the computational model for differential drive Telepresence robot navigation. This is verified using a real world Telepresence robot navigation in the laboratory environment using a new experimental framework. The contributions of this work are:

- A delay compensated non-linear state estimation approach considering continuous and uncertain time delay in measurement data. Multiple augmented states, considering delay as a model of Probability Density Function (PDF) in the form of Gaussian or Gamma distribution, are applied within the filtering method to estimate the true robot position from noisy measurements.

- A new real-environment experimental framework for Telepresence robot navigation to evaluate the performance of the proposed non-linear filter based state estimator.

- To prove the success of our approach, the proposed model was experimentally verified on a state-of-the-art differential-drive Telepresence robot in the real-environment using the proposed framework.

An overall flow diagram of the proposed model is shown in Figure 8 and described in Section 3. The overall framework is shown in Figure 2 followed by a detailed description in Section 4. The initial idea and primary results were reported in the form of conference publications [30, 31]. This paper provides detailed mathematical formulation of the proposition, introduces uncertainty in measurement delay and provides extensive experimental results and discussions. To the best knowledge of the authors, the proposed approach is first of its kind in compensating delays in differential-drive Telepresence robot navigation.

This paper is organised as follows. In Section 3.1.2, the non-linear function equations are derived. Section 3.3 introduces the methodology to deal with the delayed measurement. In Section 4, the experimental framework has presented. In Section 5, experimented results are analysed and evaluated the proposed methodology. Finally, Section 6, concludes the paper.

3. Delay compensated state estimation

3.1. Preliminaries

The proposed computational model relies on a couple of preliminaries including the kinematic model and extend Kalman filters (EKF) which has been used to develop the hypothesis and the algorithm. Therefore, it is sensible to revisit these briefly in this subsection.

3.1.1. Kinematic model of a differential drive robot

The robot used in this research was a four-wheeled differential drive Telepresence robot. Two front wheels were drive wheels and rear two wheels were castor wheels for stability. Drive wheels were controlled independently by Robot Operating Systems (ROS[2]) commands

---

[2]`www.ros.org/core-components/`
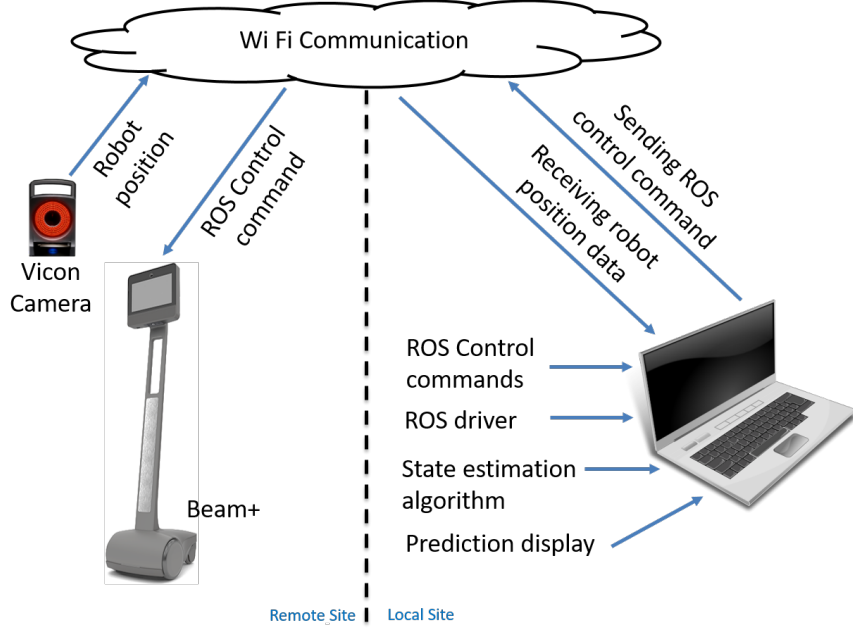
Figure 2: Experimental framework with a state-of-the-art off-the-shelve Telepresence robot Beam+. The robot was a differential drive robot which was controlled by ROS commands from a host computer through WiFi communication. The movement of the robot was captured by the multiple Vicon motion tracker.

from a host computer. The kinematic model [32] of a differential drive robot was defined as follows:

$$x_k = x_{k-1} + \Delta D_{k-1} * \cos \theta_k, \tag{1}$$

$$y_k = y_{k-1} + \Delta D_{k-1} * \sin \theta_k, \tag{2}$$

$$z_k = z_{k-1}, \tag{3}$$

$$\theta_k = \theta_{k-1} + \Delta \theta_{k-1}, \tag{4}$$

$$\Delta V_{k-1} = \frac{1}{2} * (v_{l,k} + v_{r,k}) * dt, \tag{5}$$

$$\Delta \theta_{k-1} = \frac{rw}{b} * (\omega_{l,k} - \omega_{r,k}) * dt, \tag{6}$$

where, x_k, y_k and z_k were the Cartesian coordinates of the robot, ΔD_{k-1} was the travelled distance at time step $k-1$ to k, θ_k was the angle between robot and x axis, $\Delta \theta_{k-1}$ was the rotation angle at time step $k-1$ to k, $v_{l,k}$ and $v_{r,k}$ were linear velocity of left wheel and right wheel, $\omega_{l,k}$ and $\omega_{r,k}$ were angular velocity of left wheel and right wheel, rw was the radius of the two drive wheels and dt was the sampling time.

3.1.2. Filter based state estimation equations

In this research, our aim was to estimate the true robot pose from noisy sensor measurements. The process governed by the non-linear stochastic differential equation with
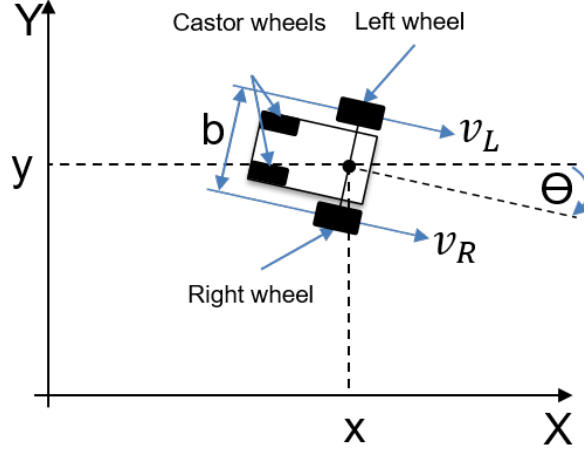
Figure 3: The Robot Kinematics in this experiment. The robot was a four-wheeled differential drive Telepresence robot. Two front wheels were drive wheels and rear two wheels were castor wheels for stability.
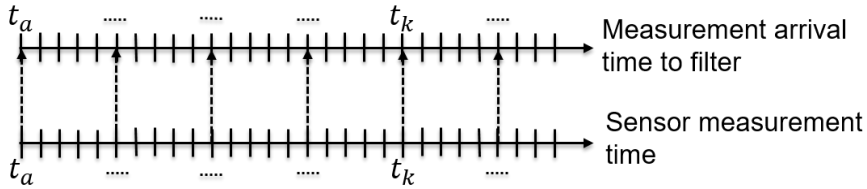

Figure 4: The figure shows an ideal case, when sensor measurement data enters into the filtering algorithm without any time delay (Figure adapted from [29]).

estimating the state vector $x \in \mathscr{R}^n$ represented as

$$x_{k+1} = f(x_k, u_k, w_k). \tag{7}$$

The measurement equation with $z \in \mathscr{R}^m$ was represented by

$$z_k = h(x_k, v_k), \tag{8}$$

where, the non linear function $f(\cdot)$ in Equation (7) relates the state at time step k to the state at step $k+1$. The non linear function $h(\cdot)$ in the measurement Equation (8) relates the state x_k to the measurement z_k. x_{k+1} represents the actual state vector including the previous state x_k, an control input u_k and the process noise w_k. z_k represents the measurement state vector including the state x_k and the measurement noise v_k. The random variables w_k and v_k represent the process and measurement noise respectively. They are assumed to be independent of each other, white, with zero mean Gaussian distributions, being Q and R the process and measurement noise covariance, respectively.

In an ideal case considering no time delay in the system, in a single time occurrence, when sensor measurement data arrives to the computer, its coincide with the measurement data at the same time step available in a Filter as shown in Figure 4. In such cases filtering

8

methods like EKF algorithm [16][33] is applied. A complete set of EKF estimation equations can be expressed as

Time update equations (Prediction):

$$\hat{x}_{k+1}^- = f(\hat{x}_k, u_k, 0), \tag{9}$$

$$P_{k+1}^- = A_k P_k A_k^T + W_k Q_k W_k^T. \tag{10}$$

In the EKF, the time update equations represent the state $\hat{x}^-$ and covariance P^-, both estimated from the time step k to the time step $k+1$. A_k and W_k are the process Jacobians at step k, and Q_k is the process noise covariance at step k.

Measurement update equations (Correction):

$$K_k = P_k^- H_k^T (H_k P_k^- H_k^T + V_k R_k V_k^T)^{-1}, \tag{11}$$

$$\hat{x}_k = \hat{x}_k^- + K_k(z_k - h(\hat{x}_k^-, 0)), \tag{12}$$

$$P_k = (I - K_k H_k) P_k^-. \tag{13}$$

In the EKF, the measurement update equations correct the state and covariance estimates with the measurement. H_k and V_k are the measurement Jacobians at step k, and R_k is the measurement noise covariance at step k.

3.2. Delay modelling
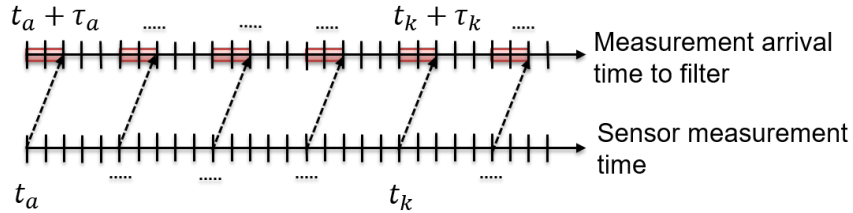
Figure 5: If the measurement data is corrupted by continuous time delay, the measurement data arrival time in the computer does not coincide with the moment when the data enters into the filtering algorithm (Figure adapted from [29]).

However, in reality, the system is assumed to be delayed. Considering time delay as continuous in nature both time steps do not coincide with each other, which produces an amount of time delay during navigation as shown in Figure 5. In such cases, the measurement equation should be redefined as [23]

$$z_k = h(x_{k-\tau_k}, v_{k-\tau_k}), \tag{14}$$

where, τ_k is the number of delayed time steps.

In our case, we assumed that the time delays τ_k are not precise due to various delay, namely, feedback delay and transmission delay and data packet drop-outs over the Internet
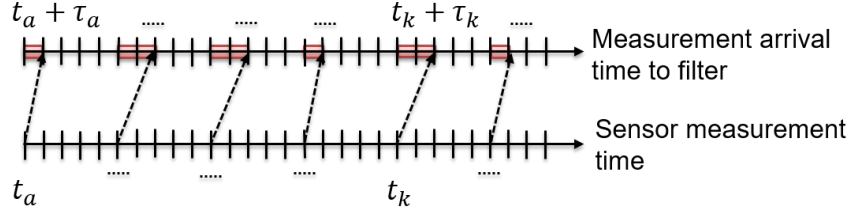
Figure 6: If the time delay is uncertain in nature and the arrival at different time step in the filtering algorithm is random (Figure adapted from [29]).

due to network congestions as discussed in Section 2.1 and hence the arrival in different filter measurement time durations Δt are random as shown in Figure 6. Therefore, it is important to model uncertain delays to obtain a consistent state estimator. Such uncertain delays are modelled here by probabilistic density functions (PDF). When the measurement data arrived at the filter, the probability that the measurement at a given time step was calculated by integrating the PDF over the time interval as shown in Figure 7. It is worth noting that one may use time stamps instead of the PDFs. However, time stamp alone is unlikely to solve the problem of state estimations as the time stamp information itself is to be delayed along with the measurements. Additionally measuring and processing individual time stamps will increase the complexity and not always necessary as the delays can be modelled using known distributions, *e.g.*, Gaussian and Gamma.
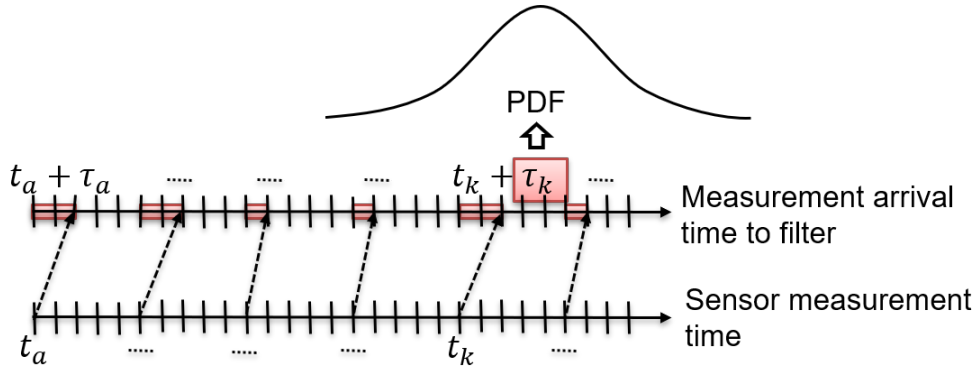

Figure 7: If the measurement data arrival is uncertain, the time delay is considered as a probabilistic density function (*e.g.*, Gaussian or Gamma). The probability of the time step in example measurement data is shown in this figure (Figure adapted from [29]).

The probability of the measurement data in k^{th} time step can be expressed as

$$\delta_k = P\left(\left(t_k - \frac{\Delta t}{2}\right) \leq t < \left(t_k + \frac{\Delta t}{2}\right)\right), \tag{15}$$
$$= \int_{t_k + \frac{\Delta t}{2}}^{t_k - \frac{\Delta t}{2}} p(t)dt,$$

where, $P(.)$ denotes probability and $p(.)$ denotes the PDF.

10

3.2.1. Delay distributions

The delay distributions have been studied in the literature and in this work we have focused on two most commonly reported PDFs, *i.e.*, (1) Gaussian and (2) Gamma distributions. The former one represents general delay modelling when delay distributions are not known [34, 35] and the latter one constitutes of Internet-based delay models when Gaussian model fails in characterising the distribution property or the distribution of the input traffic rates is non-Gaussian [36, 37, 38]. These PDFs are defined as follows:

Gaussian distribution: The probability density function of the Normal distribution or Gaussian distribution is:

$$f(x) = \frac{1}{\sigma\sqrt{2\pi}} \exp^{-\frac{1}{2}}(\frac{x-\mu}{\sigma})^2, \tag{16}$$

where the parameter μ is the mean or expectation and σ is the standard deviation of the distribution.

Gamma distribution: The probability density function in the shape-rate parametrization is

$$f(x) = \frac{\beta^{-\alpha}x^{\alpha-1}\exp(-\frac{x}{\beta})}{\Gamma(\alpha)} \quad \text{for } x > 0 \text{ and } \alpha, \beta > 0 \tag{17}$$

where $\Gamma(\alpha)$ is the Gamma function and α and β are shape and rate parameter. These parameters are related to the mean and variance of the delay by $\mu = \alpha/\beta$ and $\sigma = \beta^2/\alpha$.

While the most commonly used delay distributions are Gaussian and Gamma distributions and hence, considered in our algorithm, other probability distributions such as uniform distribution could be used to model the uncertain time delay which is outside the scope of this paper.

3.3. The algorithm

When sensor measurements are corrupted by the time delay, the current state could not be directly corrected using the current measurement, since a delayed sensor measurement was actually carrying information about a past measurement state. Here, $x(k)$ could not be corrected directly because the measurement values depend on the past measurement state $x(k - \tau)$. Therefore, the past measurement state corresponding to a delayed measurement needed to be determined before using the delayed measurement during the state estimation. The current state also needed to be corrected after correcting the appropriate past state.

3.3.1. Augmented State Extended Kalman Filter (AS-EKF)

In this research, we have used augmentation of states with EKF filter [29] for delay compensated state estimation of Telepresence robots with considering uncertain delayed sensor measurements as depicted in Figure 8. We augmented the present and past states into several augmented state vectors to estimate the robot's true position. The current measurement state which containing information of the past measurement states, directly corrects the augmented state vectors. In this way, in a delayed system, we determined the corresponding past state in the augmented state vector. After that, the past state was updated using the delayed measurement data and the current state was simultaneously
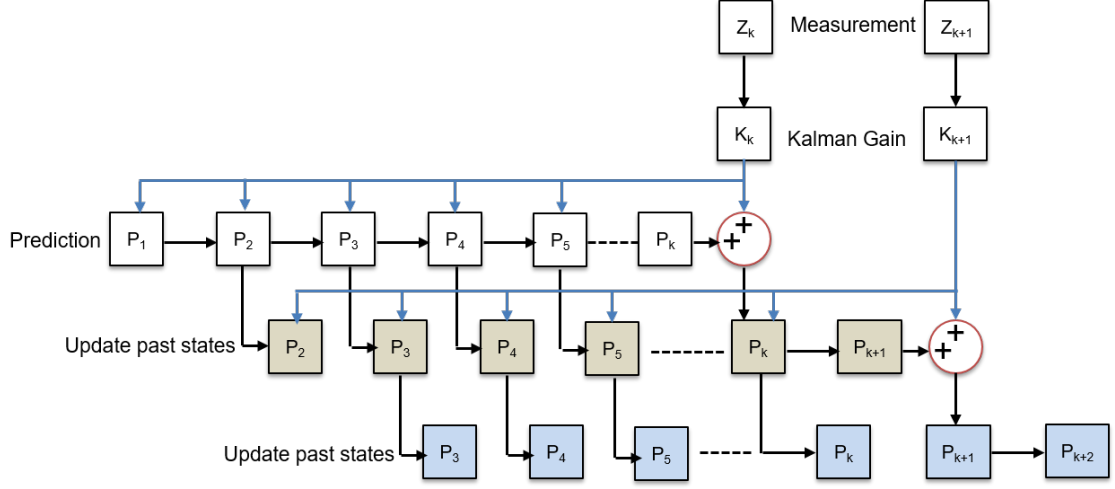
Figure 8: Flow diagram of the proposed algorithm. The diagram shows the sequence of steps involved in the AS-EKF model used in this work.

corrected in the augmented state vector. It is to be noted that firstly the algorithm considers known fixed time delay which is then extended to compensate uncertain delays using PDFs.

For one time step delay, the prediction equation was modified as

$$
\begin{bmatrix} x_{k+1} \\ x_k \end{bmatrix} = \begin{bmatrix} f(x_k, u_k, w_k) \\ x_k \end{bmatrix} \tag{18}
$$

where, $\begin{bmatrix} x_{k+1}^T & x_k^T \end{bmatrix}^T$ was the augmented state vector. The measurement equation was

$$
z_k = h \left(\begin{bmatrix} 0 & I \end{bmatrix} \begin{bmatrix} x_{k+1} \\ x_k \end{bmatrix}, v_k \right) \tag{19}
$$

where, I was the identity matrix, the current measurement z_k was used to update $\begin{bmatrix} x_{k+1}^T & x_k^T \end{bmatrix}^T$.

For multi step delays, the prediction equation defined as

$$
\begin{aligned}
\mathcal{X}_{(k+1)} &= \begin{bmatrix} f(x_k, u_k) \\ \begin{bmatrix} I & 0 & 0 & 0 \\ 0 & \ddots & 0 & \vdots \\ 0 & 0 & I & 0 \end{bmatrix} X_k \end{bmatrix} + \begin{bmatrix} w_k \\ 0 \\ \vdots \\ 0 \end{bmatrix} \\
&\equiv f(\mathcal{X}_k, \mathcal{U}_k, \mathcal{W}_k)
\end{aligned} \tag{20}
$$

where, $\mathcal{X}_{(k)}$ was the augmented state vector defined by $\begin{bmatrix} x_k^T & x_{k-1}^T & \cdots & x_{k-n}^T \end{bmatrix}^T$ and n was the maximum number of delayed time steps. The measurement equation was rewritten as
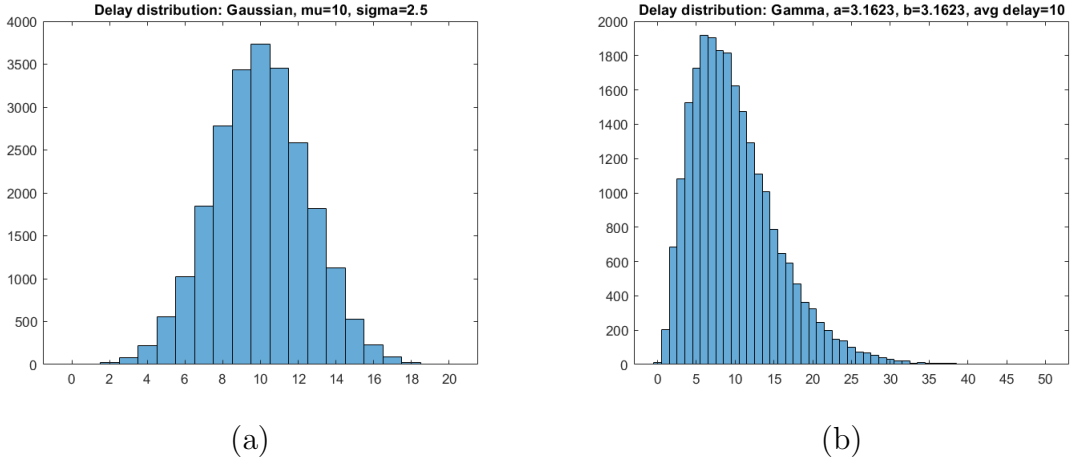
Figure 9: Histogram of delay probability density functions for average delay $\tau = 10$: (a) and (b) represent Gaussian and Gamma distributions, respectively.

$$\mathcal{Z}_k = h\left(\begin{bmatrix} 0 \\ \vdots \\ I \\ \vdots \\ 0 \end{bmatrix}^T \begin{bmatrix} x_k \\ \vdots \\ x_{k-\tau_k} \\ \vdots \\ x_{k-n} \end{bmatrix}\right) + \begin{bmatrix} 0 \\ \vdots \\ v_{k-\tau_k} \\ \vdots \\ 0 \end{bmatrix} \tag{21}$$

$$\equiv h(\mathcal{X}_k, \mathcal{V}_k)$$

where, τ_k represented the time delay, which was less than n, and I was placed at the corresponding time step $k - \tau_k$. If the time delay τ_k is known and regular, the augmented state vector can be estimated recursively via the EKF algorithm.

EKF algorithm consists prediction and measurement update stages. In the prediction stage, state prediction was carried out by the prediction equation (Equation (7)). The error covariance was propagated by the Jacobian of the prediction model and the process noise covariance(Q). The measurement update stage or measurement model was based on the prediction model and the error covariance (Equation (8)). The Jacobian of the measurement model and the measurement noise(R) were needed to obtain the Kalman gain (K). The proposed method was implemented in the augmented state vector using prediction and measurement update stages of EKF algorithm.

Dealing uncertain delays: So far our model considers known continuous delays and compensated the prediction through augmented states. However, in practice often delays are unknown (as discussed in Section 2.1) and therefore we extend the AS-EKF to handle uncertain delays. Our hypothesis is that while delay for each measurement is different, the average delay is measurable by modelling the probability of factors that introduces such delay, *e.g.*, feedback or Internet communication. In this work the modelling of uncertain

delays were done using the PDF in terms of two different delay distributions, *i.e.*, *Gaussian* and *Gamma* (as discussed in Section 3.2.1) to get a consistent state estimator. Examples of such delays, *i.e.*, Gaussian and Gamma are shown in Figure 9 (average delay $\tau = 10$).

In extending the proposed algorithm for uncertain delays, we consider such average delay (modelled by PDFs, the peaks in example figure) as continuous input to the system. This allows us to directly apply proposed AS-EKF for state estimation in uncertain scenarios. We verify this hypothesis in Section 5.2.2 by simulating various average delays for uncertain time delay scenarios. The results are promising and asserts the fact that the proposed algorithm offers a better and consistent delay compensated state estimation in both the certain and uncertain delayed system environment.

4. The framework

The proposed framework was built based on our experimental requirements, *e.g.,* state estimation of a Telepresence robot in an environment with erroneous sensor measurement due to system noise and uncertain delays (communication, processing etc.). We captured these requirements in the following subsections and described our framework which helps us to design, simulate and experiments in the controlled lab environment. An overall system architecture of our framework is depicted in Figure 2.

4.1. Requirements and Framework Components

In order to simulate various usage scenarios in our research there were some criteria needed to be fulfilled in selecting a Telepresence robot and setting up the software-hardware environment. These criteria are (1) the robot should be a mobile robot, (2) remotely operable in controlled manner, (3) have teleconferencing capabilities, and (4) a means to track robots real position.

4.1.1. Telepresence Robot

In order to have a greater control over the robot, it is sensible to chose a differential drive robot that has control individual wheels. We have used Beam+[3] which is a state-of-the-art market leading differential drive Telepresence robot in our experiments which has Telepresence capability and control through WiFi communication. Beam+ has two built-in high dynamic range cameras, LCD display and four microphone arrays with powerful audio amplifier provide a real, physical sense of presence in remote environment.

4.1.2. Odometry error correction

In a differential-drive mobile robot, incremental odometry errors are usually caused by kinematic imperfections of the robot. The two most significant errors are generated from unequal wheel diameters and the uncertainty about the effective wheelbase [39]. As the Telepresence robot used this research was a differential drive robot as described in Figure 3, it produced an enormous amount of dead-reckoning errors during navigation. Using the

---

[3]`https://suitabletech.com/products/beam`

UMBMark [39] method we have measured the dead-reckoning accuracy of the robot to find out the variance in the robot navigation and modelled in the proposed algorithm.

4.1.3. Control and Simulation Software

There are two parts of the software component in our framework: a) robot control using ROS and b) state estimation algorithmic development in MATLAB. As the latter one is commonly used for algorithmic development we only describe the robot control component using ROS. The proposed framework used ROS to navigate and control the robot. Although ROS is widely used in robotics, it challenging to control any commercial robots with a closed ecosystem using ROS. A ROS driver (a ROS node to access the hardware) was used for the experimental purposes. An existing open access robot driver ($rosbeam$[4]) was modified, customized and installed in our Beam+ robot to communicate through standard WiFi access point with a Linux based (Ubuntu) host computer. Several ROS packages that solve basic robotics problems including pose estimation, localisation in a map and mobile navigation were used in this work which includes several commands for launching nodes, introspecting topics and publishing control actions as a host to the Telepresence robot. Using ROS commands we developed algorithms to instruct the robot to navigate following the pre defined trajectory, monitor its progress, stop or redirect it along the way, and be told when it has succeeded (or failed). Also, we captured robot's positional information during the navigation.

4.1.4. Tracking Hardware

We captured robot's navigation data using Vicon motion capture system[5]. Twelve motion captured cameras were installed and calibrated in the lab which is capable of tracking robot's true state during the experiment. We have attached some retro reflective markers on the robot to represent it as a rigid body. Vicon cameras along with its software were used to record the movement of the robot. They operate in three dimensions, and tend to have high resolution, high accuracy and low variance [40].

The state estimation algorithms were implemented in a Linux based host computer. The host computer connects the Telepresence robot using ROS driver and sends ROS control command to the robot to form a $raster\text{-}scan$ navigation path and receives 3D positional data of the navigation captured by the Vicon motion cameras through standard WiFi. The motion capture data was used for two purposes: a) to verify the system path and b) to simulate other scenarios by introducing noise and delay which helped to develop the experimental setup for robust navigation.

4.2. The framework set-up and Data collection

The host computer connects the Telepresence robot using ROS driver, sends the ROS control command to the robot to form a raster-scan navigation path and receives 3D positional data of the robot navigation captured by the Vicon motion cameras through WiFi. We

---

[4]https://github.com/xlz/rosbeam
[5]https://www.vicon.com/

performed all the experiments within the robotics laboratory in our department. The experiment was to create a raster-scan path where the mobile robot travel distance was horizontal $2000mm$ and vertically $500mm$ and the orientation was 90°. We performed several runs to capture measurement data with combination of various linear velocities $(100-500mm/sec)$ and angular velocities $(100-500mm/sec)$. For all the experiments the mobile robot's starting pose was the same.

The ROS control commands were sent from the host computer over the WiFi to manoeuvre the robot creating the predefined path. Position and orientation data were recorded and used as measurement data in the proposed algorithm. The robot wheel diameters and wheelbase were modified using the correction factor calculated by dead-reckoning. On the other side, the captured robot navigation data using Vicon cameras has a low variance $(3.58mm^2)$ as reported in [40] which was also used estimating the robot's true position. It is to be noted that the Vicon captured positional data was used to simulate the noisy measurement by introducing random white noise.

Experimental parameters such as initial robot position, linear and angular velocity, correction factors for wheelbase and wheel diameter, robot variance and measurement time steps *etc.* are provided in Table 1.

Experimental parameters	Value
Initial position (x, y, z, θ)	(0,0,0,0)
Wheel radius (rw)	75 mm
Wheel base (b)	263 mm
Velocity $(v_l, v_r, \omega_l, \omega_r)$	100 mm/sec
Wheelbase correction factor (E_b)	0.9691
Wheel diameter correction factor (c_l, c_r)	0.9969, 1.0031
Robot variance $(\sigma_{\Delta\theta}^2 = \sigma_V^2)$	2.13
Vicon measurement time steps	0.01 sec
Continuous delay parameters	
Known and regular delay in time steps (τ)	[10, 15, 20, 25]
Known and regular delay in sec	[0.1, 0.15, 0.2, 0.25] sec
Uncertain delay parameters	
Gaussian parameters for uncertain delay	$\mu = [10, 15, 20, 25]$ and $\sigma = \tau/4$
Gamma parameters for uncertain delay	$\alpha = \beta = \sqrt{\tau}$

Table 1: Parameters used in the experiments.

5. Experimental results

5.1. Experimental setup

We have evaluated the proposed approach considering delayed robot navigation measurements. Using the proposed framework (described in Section 4), a raster scan robot navigation path (*design path*) was created to simulate and study our approach. Firstly, algorithm was written in ROS to remotely control the Telepresence robot Beam+. The real navigation path was monitored and tracked through the Vicon motion tracking system. As mentioned previously Vicon has extremely small error variance and hence, the Vicon output data has been considered as the actual robot path in all our experiments.

We envisage two scenarios, 1) robot navigation in a regular and known delayed environment; and 2) robot navigation in an unknown and uncertain delayed environment. In addition to that we also considered the measurement for positional data are noisy. Ideally to create such scenarios in real life one would need to arrange a set up where the local site and remote sites are physically distanced at least in order or hundreds of miles/ kilometers so that the physical communication delays are noticeable. In absence of such large geographical distance in the lab environment, we simulated the data.

Firstly, the robot velocity was assumed to have white Gaussian noise and the measurement data is accordingly also corrupted by the sensor noise. For this purposes, we have added random position noise to the Vicon output data. The noisy positional data is then arranged to insert known and unknown delays to simulate various scenarios in this work.

In real environment scenario, we cannot assume the time delay between sending a control command to the robot and the moment when the received sensor measurement data entered in the state estimator. We assumed that the measurement time delay was uncertain. In this paper, we applied state estimation algorithm to obtain the robot's true position calculating and modelling the uncertain time delay as discussed in Section 3.2.1.

5.2. Results and discussions

In order to verify our proposed approach, we initially experimented with an overall simulation followed the experiments as described in Section 5.1. A raster scan robot path was simulated using MATLAB simulations. Delay was introduced on the measurement values as a unit of time steps. Regular EKF and the proposed delay compensated approach (AS-EKF) were applied to show the effectiveness of the delay compensation approach. The results such simulation was shown in Figure 10 where the figure on the left hand side shows the complete path. The right hand figure is a zoomed version of the selected area which clearly shows regular EKF was unable to handle delay when the robot changes its direction. On contrary, as expected the AS-EKF compensated the delay and closely follows true robot path. On verification of our approach on the simulations, we performed detailed experiments on the Beam+ telepresence robot using the experiential framework (described in the following subsections).

5.2.1. Scenario I: Regular and known time delay

Considering regular and known time delay in the sensor measurement, we applied both EKF and delay compensated AS-EKF algorithms as discussed in Section 3.3. To gain an

<div align="center">(a)   (b)</div>
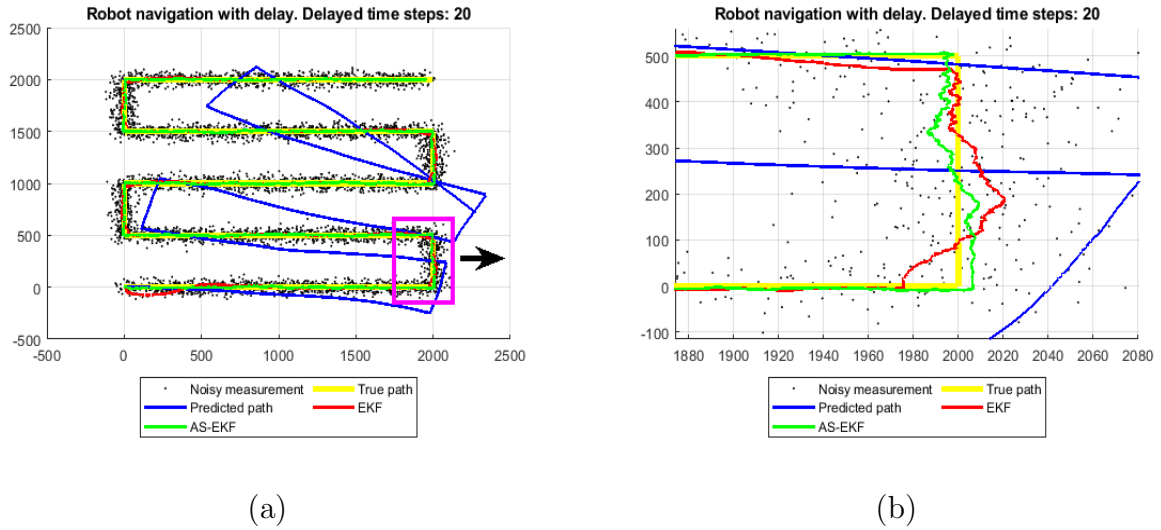
Figure 10: Comparison of EKF with AS-EKF estimated robot path with simulated time delayed measurement data. (a) overall robot navigation path; (b) zoomed version of the selected path that shows effectiveness of AS-EKF over regular EKF.

Delay	RMSE		Improvement
in time steps	EKF	AS-EKF	(%)
10	17.60	11.88	32.50
15	20.57	12.01	41.63
20	23.38	11.94	48.92
25	26.17	11.96	54.28

<div align="center">Table 2: RMSE error comparison for regular and known time delay.</div>

in-depth insight we have introduced a number of delay in time steps ($\tau = [10, 15, 20, 25]$) corresponding to delay in equivalent of $[0.1, 0.15, 0.2, 0.25]$ seconds, respectively. The delay parameters are shown in Table 1. Results for corrected navigation path (for $\tau = 10$) is shown in Figure 11. The results show that AS-EKF algorithm is reducing the linearisation error and compensating the time delay more precisely. Instead of EKF estimated path, the AS-EKF estimated path is more close to the robot control path.

In order to capture performance for delay compensation, we calculated the error in terms of root mean square error (RMSE) between the Vicon measurement (absolute robot path) and estimated path by EKF and AS-EKF, respectively, with respect to measurement time steps. The results for complete paths are shown in Figure 12 and average RMSE errors for entire paths are reported in Table 2.

The results show that with the increase of number of delayed steps in the measurement data, the performance of the EKF algorithm proportionally decreases as the time delay in
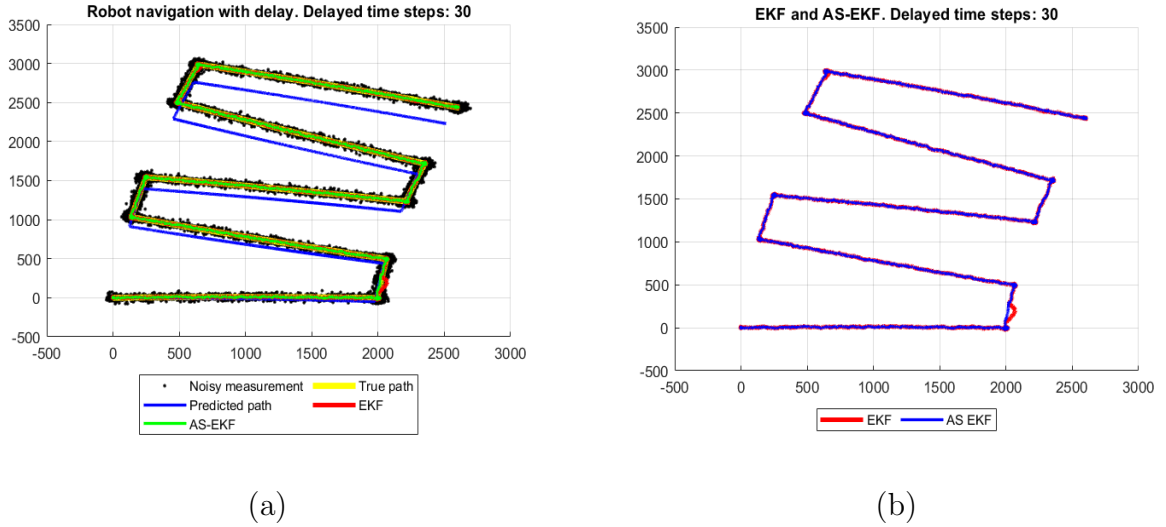
Figure 11: Comparison of EKF with AS-EKF estimated robot path with time delayed measurement data. (a) Overall comparison; (b) Comparison between EKF and AS-EKF.

the measurement data degraded the state estimation accuracy of the algorithm. AS-EKF significantly reduces the error and maintained at the same level by compensating the error introduced by the delay. In our experiments we have achieved improvements of 33% to 54% when considering the delay compensated AS-EKF as opposed to regular EKF.

5.2.2. Scenario II: Uncertain time delay

As mentioned earlier sections, regular and known time delays are rare in real life environments. Therefore, we consider scenarios with uncertain time delays as discussed in Section 3.2. As previous study shows uncertain delays can be modelled using the probability density functions (PDF), such as, Gaussian and Gamma distributions, we considered both distributions in simulating delays within measurement values. Random delays with averages similar to the known regular time delays are introduced in respective distributions and the distribution parameters were calculated accordingly. The distribution parameters are reported in Table 1 and example plots of positional error due to uncertain delay with respect to time steps for both Gaussian and Gamma distributions are shown in Figure 13 (average time delay $\tau = 10$). As described in Section 3.3.1 (*Dealing uncertain delays*), we considered the average delays as input to the system and estimated states using the proposed AS-EKF algorithm. Similar to known delays the results of AS-EKF for uncertain delays were compared against state estimation using EKF only that does not considers delay compensation.

The results for delay with Gaussian and Gamma distributions are shown in Figure 14 and Figure 15, respectively. Similar to the known and regular delay, we calculated the error between the estimated path and Vicon measurements (absolute robot path) and compared for EKF without considering delay compensation and AS-EKF that compensated the delay by assuming the average delay in these scenarios. The RMSE error for Gaussian and Gamma distributed delays are shown in Table 3 and Table 4, respectively. In both cases we have

19

(a) $\tau = 10$.

(b) $\tau = 15$.

(c) $\tau = 20$.

(d) $\tau = 25$.
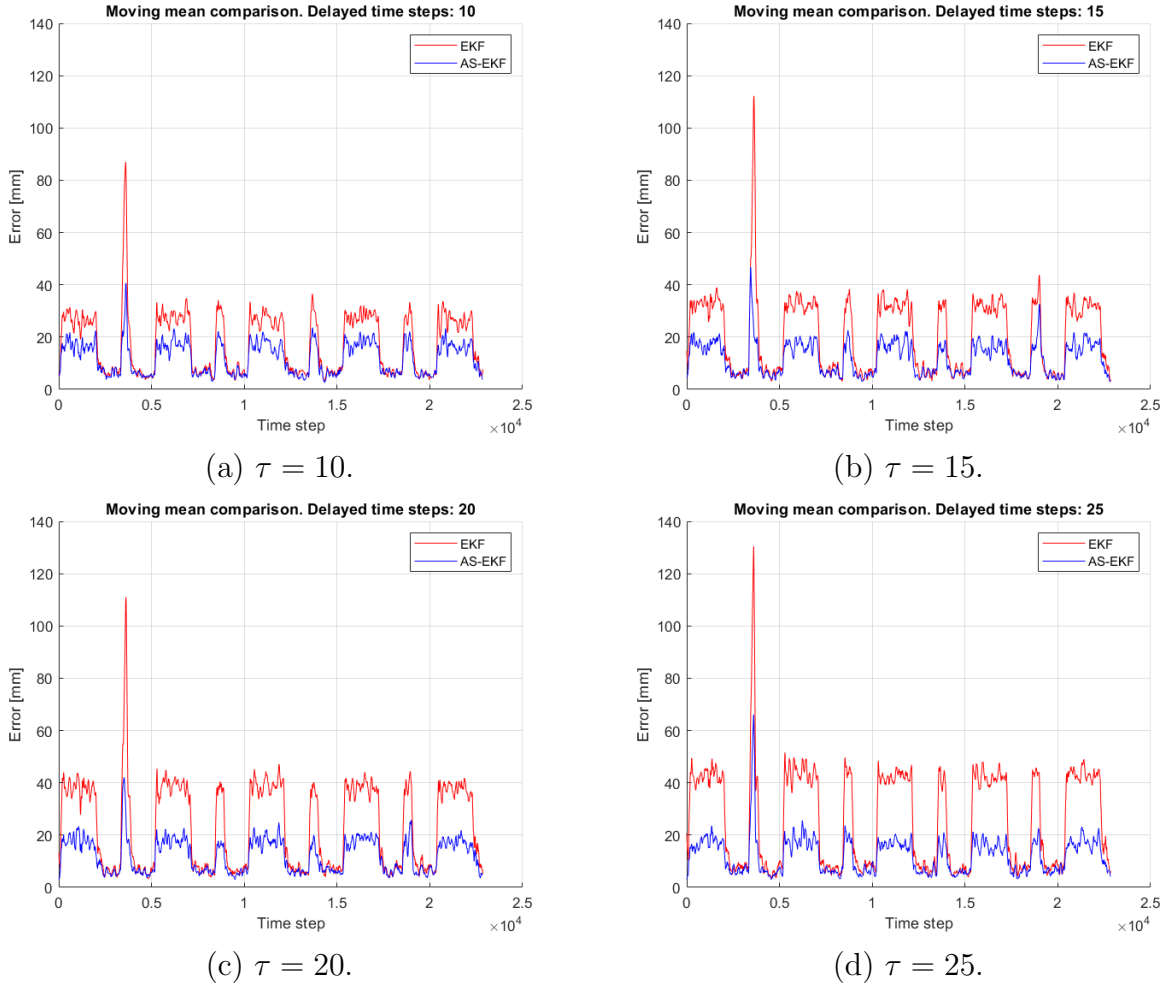
Figure 12: RMSE error comparison for regular and known time delay. The red line and blue line represent the RMSE error of EKF and AS-EKF estimation.

observed more than 50% improvements.

Finally we have compared the estimation error for various scenarios, *e.g.,* regular and known delay, uncertain delay with Gaussian and Gamma distributions. The results are shown in Figure 16 for $\tau = [10, 20]$. We have also compared the RMSE errors and reported in Figure 17.

5.3. Discussions

We have conducted all experiments using our proposed experimental framework. The delay compensated state estimation approach successfully estimated the robot's true position during navigation and compensated the time delay from the noisy measurement data as described before. During the experiments we have used the robot's original hardware parameters.

Comparing with existing EKF techniques estimating robot's true position, we have shown
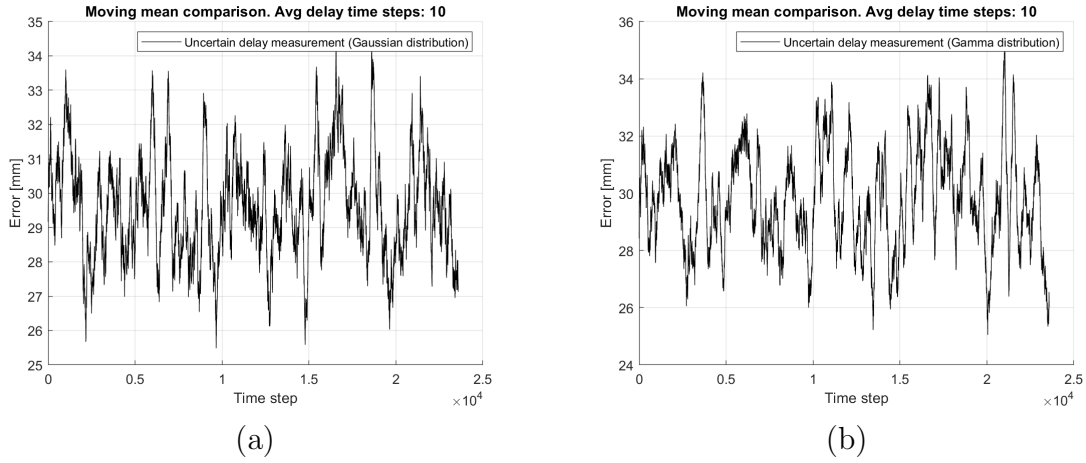
Figure 13: Positional error due to uncertain delay with average delay $\tau = 10$: (a) and (b) represent delay modelled using Gaussian and Gamma distributions, respectively.

Average delay	RMSE		Improvement
in time steps	EKF	AS-EKF	(%)
10	19.11	13.22	30.79
15	31.54	13.08	39.29
20	23.62	12.81	45.77
25	26.67	13.07	50.99

Table 3: RMSE error comparison for uncertain time delays with Gaussian distribution.

that our delay compensated AS-EKF based approach improves the estimation of robot positions in the scenarios with delayed noisy sensor measurements. The observation indicates best results are achieved by the delay compensated AS-EKF when the delay is regular and known. Although, it is not as good as the known delay scenario, the proposed algorithm works well for uncertain delays provided the average delay is known which can be estimated empirically. We also observed the algorithm works relatively better for Gamma distribution. This is due to the fact that the Gamma distribution in our experiments are relatively skewed towards left, *i.e.,* smaller delays.

6. Conclusions

In this paper, a delay compensated state estimation approach for a Telepresence robot with uncertain delayed navigation measurement was presented. EKF combining with augmented state model was successfully executed estimating actual robot position modelling known and uncertain time delays in the robot navigation. The uncertainty of the time delays were modelled by considering PDF in terms of Gaussian and Gamma distributions. The
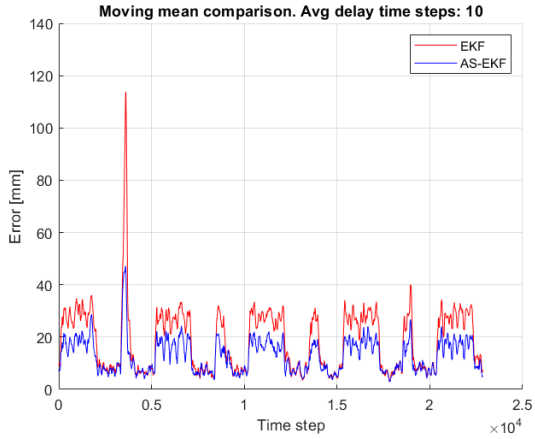
(a) Average $\tau = 10$.
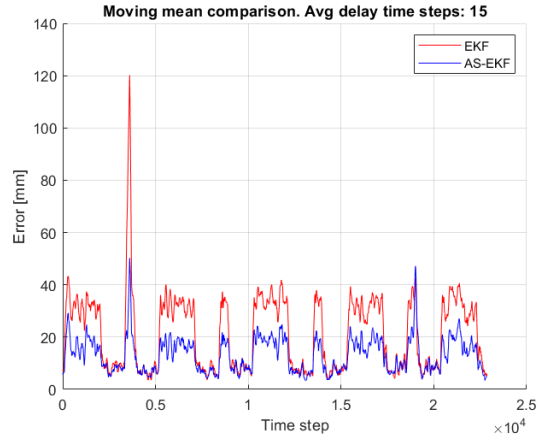
(b) Average $\tau = 15$.
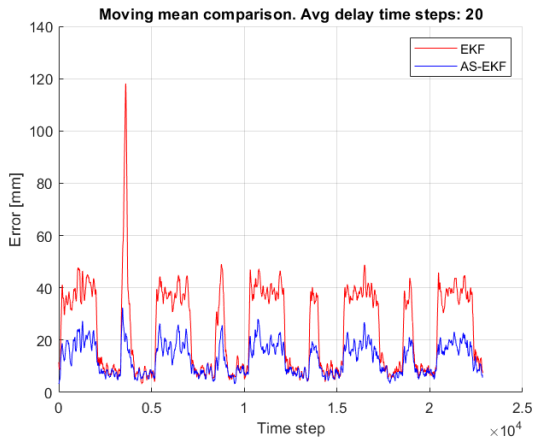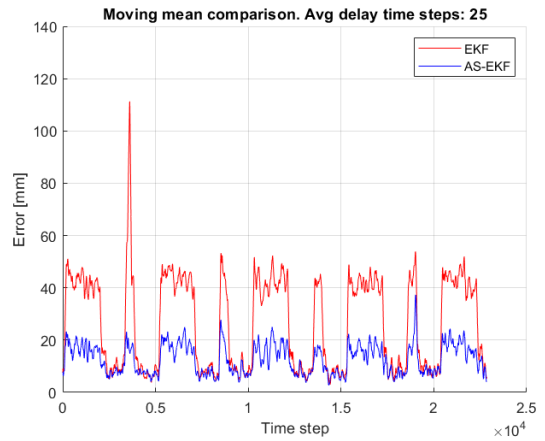
**(c)** Average $\tau = 20$.

(d) Average $\tau = 25$.

Figure 14: RMSE error comparison for uncertain time delay with Gaussian distribution. The red line and blue line represent the RMSE error of EKF and AS-EKF estimation respectively.

robot paths estimated by the delay compensated AS-EKF algorithm and EKF algorithm that does not consider any delay, are compared to evaluate the improvement in navigation performance. The proposed model was experimentally implemented in simulation and verified in the real environment experimental framework with a state-of-the-art commercial Telepresence robot. As a future work, we intend to build a predictive display to address the challenges of visual mismatch between the predicted state and actual navigation state of the robot. The predictive display is envisaged to show the immediate estimated robot path while the robot is navigating under delayed network.

Acknowledgements

22
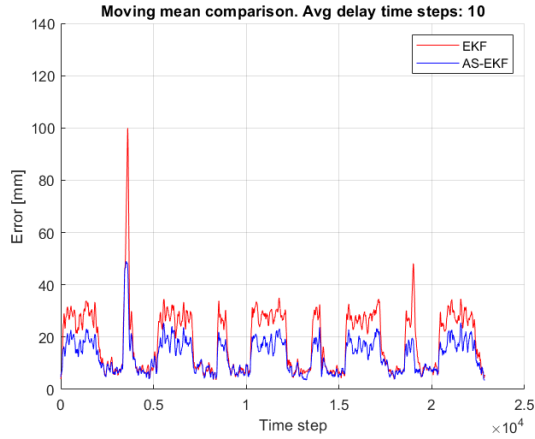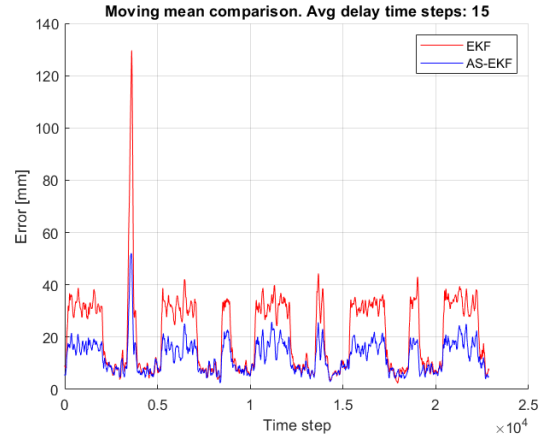
(a) Average $\tau = 10$.

(b) Average $\tau = 15$.
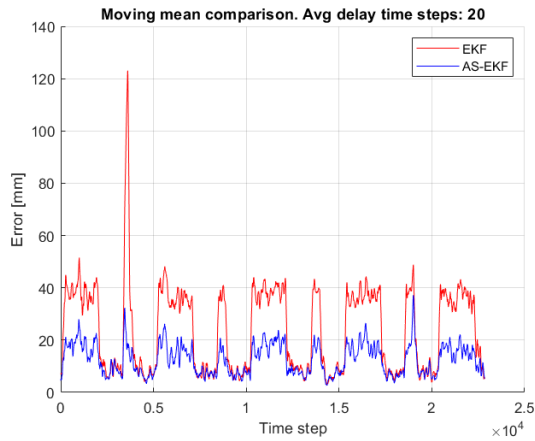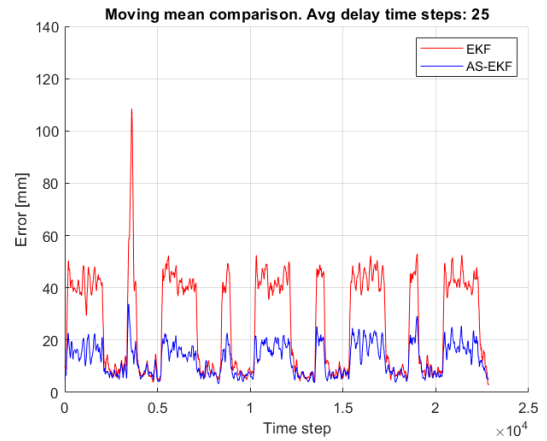

(c) Average $\tau = 20$.

(d) Average $\tau = 25$.

Figure 15: RMSE error comparison for uncertain time delay with Gamma distribution. The red line and blue line represent the RMSE error of EKF and AS-EKF estimation respectively.

[1] K. M. Tsui, M. Desai, H. A. Yanco, C. Uhlik, Exploring use cases for telepresence robots, in: Proceedings of the 6th international conference on Human-robot interaction, ACM, 2011, pp. 11–18.

[2] R. Held, N. Durlach, Telepresence, time delay and adaptation, Pictorial communication in virtual and real environments (1991) 232–246.

[3] K. Kawabata, T. Sekine, T. Suzuki, Mobile robot teleoperation system utilizing a virtual world, Advanced Robotics 15 (1) (2001) 1–16. doi:10.1163/156855301750095550.

[4] M. Colledanchise, D. V. Dimarogonas, P. Ogren, Robot navigation under uncertainties using event based sampling, in: Annual Conference on Decision and Control (CDC), IEEE, 2014, pp. 1438–1445.

[5] R. J. Anderson, M. W. Spong, Bilateral control of teleoperators with time delay, IEEE Transactions on Automatic Control 34 (5) (1989) 494–501.

[6] I. Vittorias, J. Kammerl, S. Hirche, E. Steinbach, Perceptual coding of haptic data in time-delayed teleoperation, in: World Haptics 2009 - Third Joint EuroHaptics conference and Symposium on Haptic Interfaces for Virtual Environment and Teleoperator Systems, 2009, pp. 208–213.

[7] J. Funda, T. S. Lindsay, R. P. Paul, Teleprogramming: Toward delay-invariant remote manipulation, Presence: Teleoperators and Virtual Environments 1 (1) (1992) 29–44. doi:10.1162/pres.1992.1.1.29.

Average delay	RMSE		Improvement
in time steps	EKF	AS-EKF	(%)
10	18.53	12.85	30.67
15	21.16	12.78	39.61
20	24.09	12.71	47.24
25	26.60	12.65	52.46

Table 4: RMSE error comparison for uncertain time delay with Gamma distribution.


(a) (b)
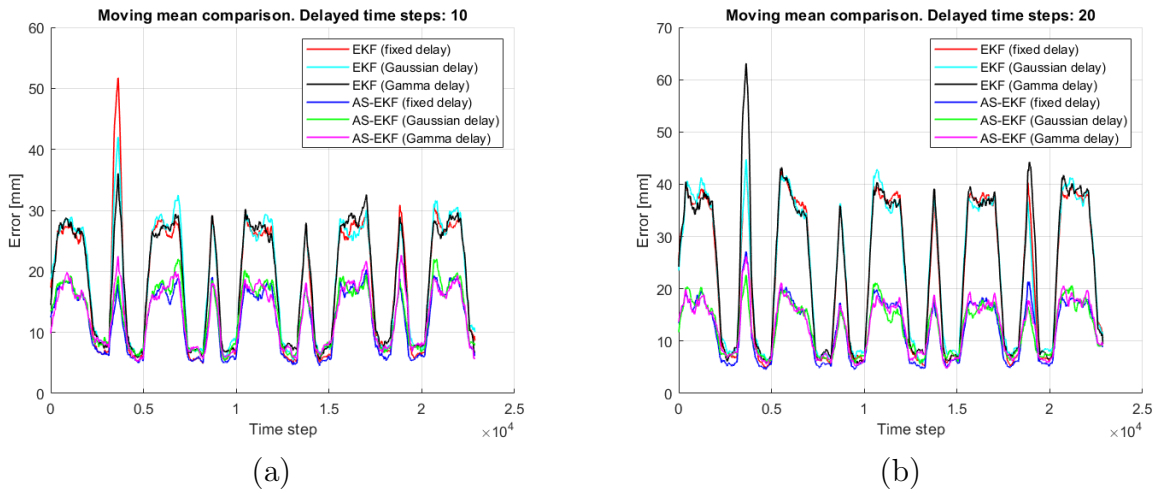
Figure 16: RMSE error comparison of EKF and AS-EKF estimation. (a) The red, cyan and black line represent the RMSE error of EKF estimation for fixed delay, uncertain delay with Gaussian distribution and Gamma distribution respectively. (b) The blue, green and magenta line represent the RMSE error of AS-EKF estimation for fixed delay, uncertain delay with Gaussian distribution and Gamma distribution respectively.

[8] M. Hernando, E. Gambao, A robot teleprogramming architecture, in: Proceedings 2003 IEEE/ASME International Conference on Advanced Intelligent Mechatronics (AIM 2003), Vol. 2, 2003, pp. 1113–1118.

[9] K. Brady, T. . Tarn, Internet-based teleoperation, in: Proceedings 2001 ICRA. IEEE International Conference on Robotics and Automation (Cat. No.01CH37164), Vol. 1, 2001, pp. 644–649.

[10] A. Mora, D. G. Axelson, M. Chacin, K. Nagatani, K. Yoshida, Assisted teleoperated navigation system based on 3d mapping, in: 1st Annual IEEE Systems Conference., IEEE, 2007, pp. 1–6.

[11] H. Hu, C. Quintero, H. Sun, M. Jagersand, On-line reconstruction based predictive display in unknown environment, in: Robotics and Automation (ICRA), 2015 IEEE International Conference on, IEEE, 2015, pp. 4446–4451.

[12] K. Natori, T. Tsuji, K. Ohnishi, A. Hace, K. Jezernik, Time-delay compensation by communication disturbance observer for bilateral teleoperation under time-varying delay, IEEE Transactions on Industrial Electronics 57 (3) (2010) 1050–1062.

[13] A. K. Bejczy, W. S. Kim, S. C. Venema, The phantom robot: predictive displays for teleoperation with time delay, in: Proceedings., IEEE International Conference on Robotics and Automation, Vol. 1,
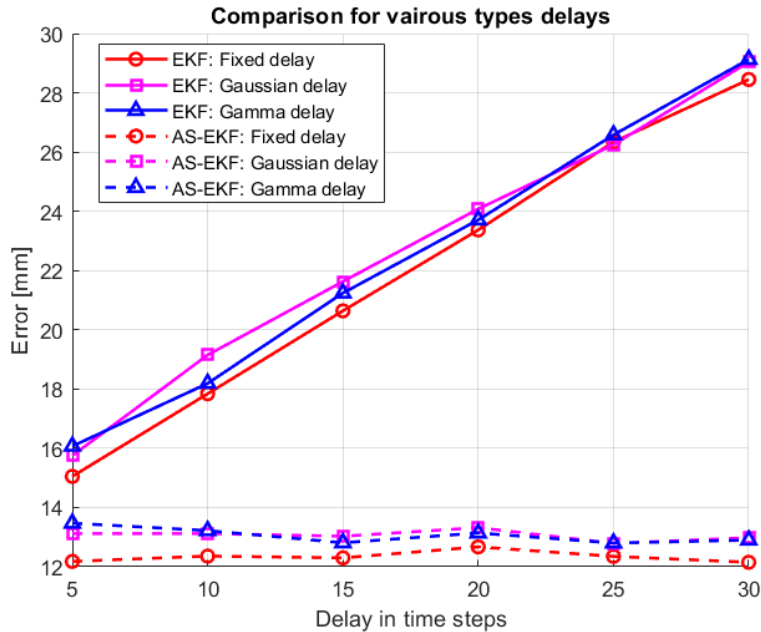
Figure 17: RMSE error comparison of EKF and AS-EKF for fixed delay and uncertain time delay with Gaussian and Gamma distribution respectively. The comparison is done for different delayed time steps. The red, magenta and blue line represent the RMSE error of EKF estimation and the dotted-line represent AS-EKF estimation respectively.

1990, pp. 546–551.

[14] J. Kikuchi, K. Takeo, K. Kosuge, Teleoperation system via computer network for dynamic environment, in: Proceedings. 1998 IEEE International Conference on Robotics and Automation (Cat. No.98CH36146), Vol. 4, 1998, pp. 3534–3539.

[15] E. Slawiski, V. Mut, L. Salinas, S. Garca, Teleoperation of a mobile robot with time-varying delay and force feedback, Robotica 30 (1) (2012) 6777. `doi:10.1017/S0263574711000427`.

[16] S. Thrun, W. Burgard, D. Fox, Probabilistic Robotics (Intelligent Robotics and Autonomous Agents), The MIT Press, 2005.

[17] A. H. Jazwinski, Stochastic processes and filtering theory, Courier Corporation, 2007.

[18] I. Karafyllis, M. Krstic, Predictor feedback for delay systems: Implementations and approximations, Springer, 2017.

[19] B. Zhou, Truncated predictor feedback for time-delay systems, Springer, 2014.

[20] Y. Bar-Shalom, Update with out-of-sequence measurements in tracking: exact solution, IEEE Transactions on Aerospace and Electronic Systems 38 (3) (2002) 769–777. `doi:10.1109/TAES.2002.1039398`.

[21] Y. Bar-Shalom, H. Chen, M. Mallick, One-step solution for the multistep out-of-sequence-measurement problem in tracking, IEEE Transactions on Aerospace and Electronic Systems 40 (1) (2004) 27–37. `doi:10.1109/TAES.2004.1292140`.

[22] T. D. Larsen, N. A. Andersen, O. Ravn, N. K. Poulsen, Incorporation of time delayed measurements in a discrete-time kalman filter, in: Proceedings of the 37th IEEE Conference on Decision and Control, Vol. 4, 1998, pp. 3972–3977. `doi:10.1109/CDC.1998.761918`.

[23] M. Bak, T. D. Larsen, M. Norgaard, N. A. Andersen, N. Poulsen, O. Ravn, Location estimation using delayed measurements, in: 5th International Workshop on Advanced Motion Control, 1998. AMC '98-Coimbra, 1998, 1998, pp. 180–185. `doi:10.1109/AMC.1998.743533`.

[24] S. Challa, R. J. Evans, X. Wang, A bayesian solution and its approximations to out-of-sequence mea-

surement problems, Information Fusion 4 (3) (2003) 185 – 199. doi:https://doi.org/10.1016/
S1566-2535(03)00037-X.

[25] R. Van Der Merwe, E. A. Wan, S. Julier, Sigma-point kalman filters for nonlinear estimation and sensor-
fusion: Applications to integrated navigation, in: Proceedings of the AIAA Guidance, Navigation and
Control Conference, 2004, pp. 16–19.

[26] S. J. Julier, J. K. Uhlmann, Fusion of time delayed measurements with uncertain time delays, in:
Proceedings of the 2005, American Control Conference., Vol. 6, 2005, pp. 4028–4033. doi:10.1109/
ACC.2005.1470607.

[27] J. Hu, Z. Wang, F. E. Alsaadi, T. Hayat, Event-based filtering for time-varying nonlinear systems
subject to multiple missing measurements with uncertain missing probabilities, Information Fusion 38
(2017) 74–83.

[28] L. Zou, Z. Wang, Q.-L. Han, D. Zhou, Recursive filtering for time-varying systems with random access
protocol, IEEE Transactions on Automatic Control 64 (2) (2018) 720–727.

[29] M. Choi, J. Choi, W. Chung, State estimation with delayed measurements incorporating time-delay
uncertainty, IET Control Theory and Applications 6 (2012) 2351–2361(10).

[30] B. Das, G. Dobie, S. G. Pierce, State estimation of delays in telepresence robot navigation using
bayesian approaches, in: 19th Annual Conference, Towards Autonomous Robotic Systems Conference
(TAROS), 2018.

[31] B. Das, G. Dobie, S. G. Pierce, AS-EKF: a delay aware state estimation technique for telepresence
robot navigation, in: IEEE International Conference on Robotic Computing (IRC), 2019.

[32] E. Ivanjko, M. Vasak, I. Petrovic, Kalman filter theory based mobile robot pose tracking using occu-
pancy grid maps, in: International Conference on Control and Automation (ICCA2005), Vol. 2, 2005,
pp. 869–874.

[33] G. Welch, G. Bishop, An introduction to the kalman filter, Tech. rep. (1995).

[34] T. T. Andersen, H. B. Amor, N. A. Andersen, O. Ravn, Measuring and modelling delays in robot
manipulators for temporally precise control using machine learning, in: 2015 IEEE 14th International
Conference on Machine Learning and Applications (ICMLA), pp. 168–175.

[35] R. Oboe, P. Fiorini, Issues on internet-based teleoperation, IFAC Proceedings Volumes 30 (20) (1997)
591–597.

[36] D. Chen, X. Fu, W. Ding, H. Li, N. Xi, Y. Wang, Shifted gamma distribution and long-range prediction
of round trip timedelay for internet-based teleoperation, in: 2008 IEEE International Conference on
Robotics and Biomimetics, 2009, pp. 1261–1266.

[37] Kim, S., Lee, J. Y., Sung, D. K., A shifted gamma distribution model for long-range dependent internet
traffic, IEEE Communications Letters 7 (3) (2003) 124–126.

[38] J. Hua, Y. Cui, Y. Yang, H. Li, Analysis and prediction of jitter of internet one-way time-delay for
teleoperation systems, in: 2013 11th IEEE International Conference on Industrial Informatics (INDIN),
2013, pp. 612–617.

[39] J. Borenstein, L. Feng, UMBmark: A benchmark test for measuring odometry errors in mobile robots,
in: Mobile Robots X, Vol. 2591, International Society for Optics and Photonics, 1995, pp. 113–125.

[40] R. Summan, S. Pierce, C. Macleod, G. Dobie, T. Gears, W. Lester, P. Pritchett, P. Smyth, Spatial
calibration of large volume photogrammetry based metrology systems, Measurement 68 (2015) 189 –
200. doi:https://doi.org/10.1016/j.measurement.2015.02.054.